nature chemistry

Article

https://doi.org/10.1038/s41557-023-01340-9

A crystalline aluminium–carbon-based ambiphile capable of activation and catalytic transfer of ammonia in non-aqueous media

Received: 19 October 2022

Accepted: 31 August 2023

Check for updates

Felix Krämer [1], Jan Paradies [2], Israel Fernández [3] & Frank Breher [1]

Despite recent achievements in the field of frustrated Lewis pairs (FLPs) for small molecule activations, the reversible activation and catalytic transformations of N–H-activated ammonia remain a challenge. Here we report on a rare combination of an aluminium Lewis acid and a carbon Lewis base. A so-called hidden FLP consisting of a phosphorus ylide featuring an aluminium fragment in the *ortho* position of a phenyl ring scaffold is introduced. Although the formation of the Lewis acid/base adduct is observed in the solid state, which at first glance leads to formally quenched FLP reactivity, we show that the title compound readily reacts with non-aqueous ammonia thermoneutrally and splits the N–H bond reversibly at ambient temperature. In addition, NH_3 transfer reactions mediated by a main-group catalyst are presented. This proof-of-principle study is expected to initiate further activities in utilizing N–H-activated ammonia as a readily available, atom-economical nitrogen source.

The hydroamination of non-activated alkenes with ammonia (NH_3) remains one of the main goals in catalysis[1]. This is because the formation of stable Lewis acid/base adducts with transition metal complexes[2] and the high gas-phase bond dissociation free energy of 99.4 kcal mol^{-1} of the N–H bond[3] make NH_3 activation a challenging endeavour[4–17]. Non-metallic compounds that mimic the reactivity of transition metal complexes have attracted considerable interest[18–21]. In 2007, Bertrand and co-workers reported the first metal-free activation of NH_3 using (alkyl)(amino)carbenes[22]. Just recently, the activation of ammonia by single-electron transfer from a dithiolene zwitterion or Bi(II) complex was reported[23,24]. Furthermore, Goicoechea and co-workers recently described the thermoneutral and reversible splitting of ammonia with a geometrically constrained phosphine, but so far, catalytic transformations of N–H-activated ammonia have remained unprecedented[25].

Since its first report, the use of so-called frustrated Lewis pairs (FLPs), consisting of sterically hindered Lewis acids and Lewis bases to prevent adduct formation in the activation of small molecules, has increased considerably[26–31]. Notwithstanding these achievements, ambiphilic molecules are promising candidates for splitting highly stable bonds, for example, N–H bonds in NH_3. B/P-based FLPs have been used for inter- and intramolecular hydroaminations of alkynes with secondary amines[32,33]. In addition quantum chemical studies present FLPs as promising candidates in the dehydrogenation of ammonia borane involving N–H bond activation[34,35]. However, the combination of an aluminium-based Lewis acid and carbon-based Lewis base is uncommon in the field of FLP chemistry. Phosphorus ylides are useful carbon Lewis bases for the stabilization of highly reactive compounds[36–39]. Therefore, the cooperative action of an aluminium Lewis acid and a Lewis basic phosphorus ylide appears to be a promising approach for achieving the challenging N–H bond activation.

Results and discussion

Synthesis and characterization

We report herein the synthesis of the Al/C-based ambiphile (2-{Al*t*-Bu_2}-C_6H_4)Ph_2PCMe_2 (**2**) and its application in the activation and transfer of NH_3. For the preparation of the title compound **2**, the *ortho*-lithiated ylide (2-Li-C_6H_4)Ph_2PCMe_2 (**1**) was generated by reaction of the readily available ylide Ph_3PCMe_2 with *t*-BuLi in toluene (Fig. 1a)[40]. The highly reactive and air- and moisture-sensitive intermediate **1** precipitates

[1]Institute of Inorganic Chemistry, Karlsruhe Institute of Technology, Karlsruhe, Germany. [2]Chemistry Department, Paderborn University, Paderborn, Germany. [3]Departamento de Química Orgánica I, Facultad de Ciencias Químicas and Centro de Innovación en Química Avanzada, Universidad Complutense de Madrid, Madrid, Spain. e-mail: breher@kit.edu

https://doi.org/10.1038/s41557-023-01340-9

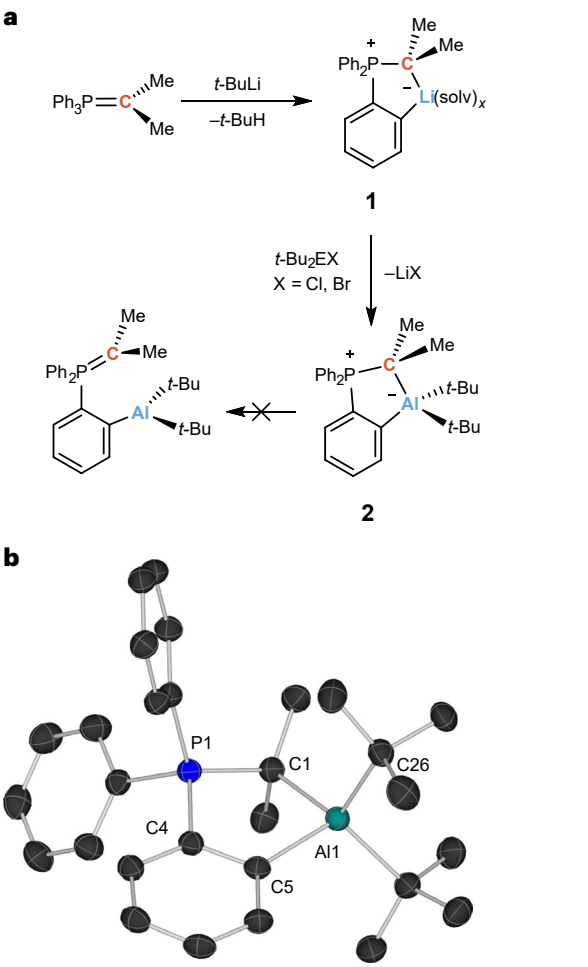

Fig. 1 | Synthesis of the aluminium–carbon-based ambiphile 2. a, Synthesis of **1** from the phosphorus ylide Ph_3PCMe_2 with *t*-BuLi and subsequent synthesis of **2** with $t\text{-}Bu_2AlX$ (X = Cl or Br) in toluene at RT. **b**, The molecular structure of **2** in the solid state (ellipsoids drawn at the 30% probability level). The hydrogen atoms are omitted for clarity. Selected bond lengths (Å) and angles (°): P1–C1 = 1.800(2), C1–Al1 = 2.118(2), C5–Al1 = 2.019(2); P1–C1–Al1 = 102.98(10).

from the reaction mixture and can be isolated as a yellow powder in 47% yield by filtration and drying in high vacuum.

The ^{7}Li nuclear magnetic resonance (NMR) at δ_{7Li} = 4.3 ppm (C_6D_6) agrees very well with the reported one of the closely related compound (2-Li-C_6H_4)Ph_2PCH_2 investigated by Sundermeyer[41]. Similarly consistent are the ^{31}P NMR chemical shifts. Compound **1** shows a signal at δ_{31P} = 21.1 ppm and is thus 10 ppm high-field shifted with respect to (2-Li-C_6H_4)Ph_2PCH_2, which follows the trend observed for the unsubstituted ylides Ph_3PCH_2 (δ_{31P} = 20.6 ppm) and Ph_3PCMe_2 (δ_{31P} = 9.4 ppm). To access the target compound **2**, **1** was reacted with $t\text{-}Bu_2AlX$ (X = Cl or Br) in toluene (Fig. 1a). After recrystallization from hexane, **2** was isolated as colourless crystals in 66% yield (Fig. 1b, space group $P2_1/n$). In crystalline form, **2** can be stored for days on the laboratory bench without any sign of decomposition.

The P1–C1 bond (1.800(2) Å) in **2** is elongated by about 10 pm compared with the α-functionalized ylides $Ph_3PC(Me)BEt_2$ (1.717(3) Å) or $Ph_3PC(R^1)ER^2_2Cl$ (E = Si or Ge with 1.682(2)–1.706(2) Å), indicating a lower double-bond character of this bond[37,42]. When compared with the average bond lengths for P–C single (1.87 Å) and P=C double bonds (1.67 Å), the P1–C1 bonds are closer in value to the single bond[43]. This observation is not surprising when considering the Lewis acidic character of the Al fragments. The detected C1–Al1 distance of 2.118(2) Å and the short C5–Al1 (2.019(2) Å) distance to the bridging phenylene ring further support the findings. The P1–C1–Al1 angle of 102.98(10)° slightly deviates from the ideal tetrahedral angle of 109.4°. The ylidic CMe_2 fragment at C1 is tilted by Φ = 27° from the plane spanned by the atoms Al1, C5, C4 and P1. Overall, the crystal structure clearly shows that the closed five-membered ring form of **2** (Fig. 1a) is the dominant resonance structure in the solid state.

N–H bond activation

Surprisingly, although the open form of **2** is, according to our density functional theory calculations, 37.5 kcal mol^{-1} higher in energy (Supplementary Information Fig. 33) and could not be observed experimentally, **2** reacted cleanly with the N–H bond when exposed to 1 atm of NH_3 (Fig. 2a). The reaction product **3** was unequivocally characterized by X-ray

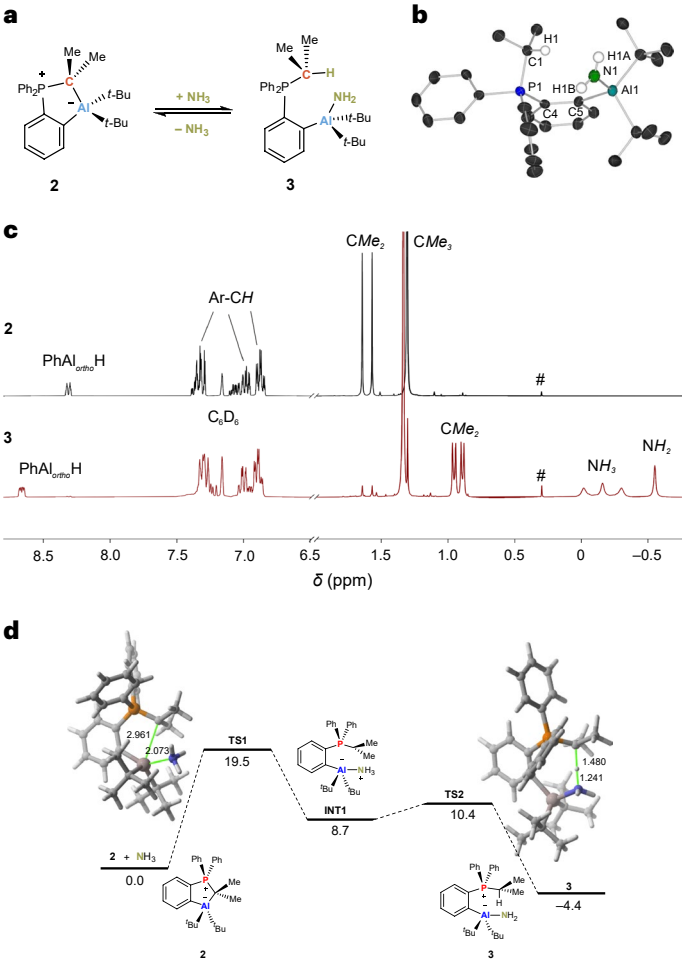

Fig. 2 | Reversible N–H activation of ammonia. a, The reversible reaction of the aluminium–carbon-based ambiphile **2** with NH_3 in benzene at RT. **b**, The molecular structure of **3** in the solid state (ellipsoids drawn at the 30% probability level). The hydrogen atoms (except the NH_2 and ylidic protons) are omitted for clarity. Selected bond lengths (Å) and angles (°): P1–C1 = 1.8237(12), N1–Al1 = 1.8494(12), C5–Al1 = 2.0766(12); C5–N1–Al1 = 110.97(5). **c**, Stacked ^{1}H NMR spectra of **2** and the ammonia activation product **3** in C_6D_6 (the hash symbol denotes grease). As can clearly be seen, a new set of signals arise in the ^{1}H NMR spectra of **3** accompanied by the decreased intensity of the signals for **2**. **d**, Computed profile (PCM(benzene)-M06-2X/def2-TZVPP//PCM(benzene)-M06-2X/def2-SVP level) for the stepwise reaction of **2** with NH_3. Relative free energies (ΔG, at 298 K) and bond distances are given in kcal mol^{-1} and angstroms, respectively. The transformation begins with the coordination of NH_3 to the aluminium atom, followed by cleavage of the C_{ylide}–Al bond. The computed reaction barrier of only 19.5 kcal mol^{-1} for transition state **TS1** is compatible with a process occurring at RT. Via **TS2**, the activation product **3** is formed in a –4.4 kcal mol^{-1} exergonic transformation.

https://doi.org/10.1038/s41557-023-01340-9

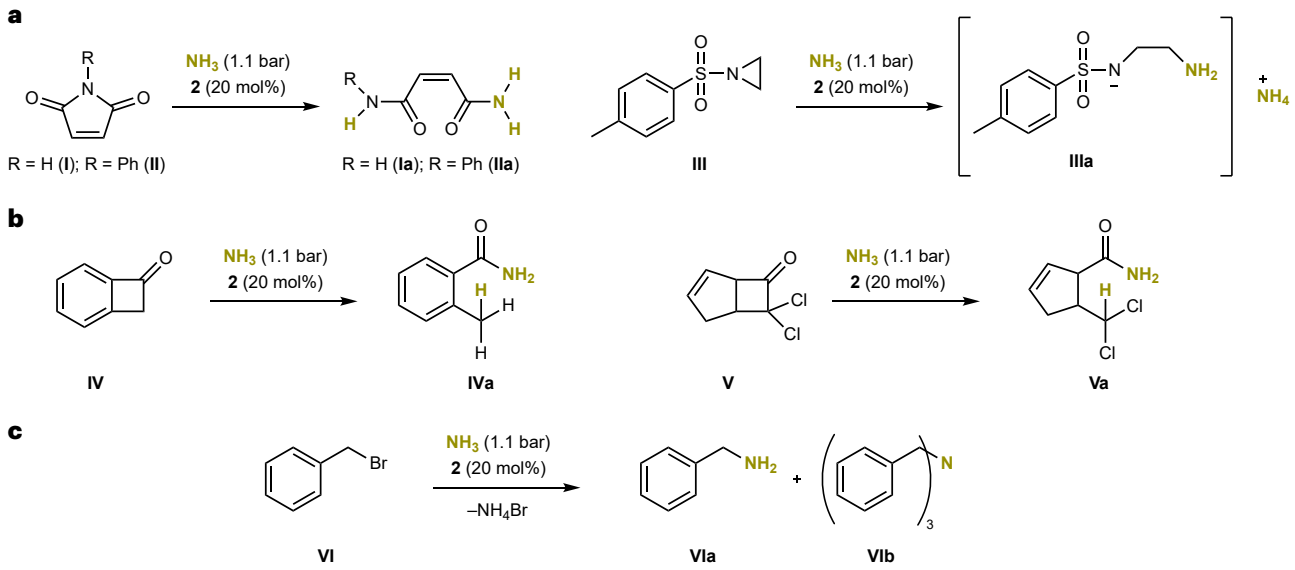

Fig. 3 | Catalytic ammonia transfer reactions in benzene at RT (p = 1.1 bar; 20 mol% compound 2). **a**, Catalytic ammonia transfer to maleimides **I** and **II** forming the linear products **Ia** and **IIa** by ring opening, and ring-opening transfer of ammonia to tosylaziridine **III**, leading to **IIIa** after subsequent deprotonation to the ammonium salt. **b**, Benzocyclobutenone (bicyclo[4.2.0]octa-1,3,5-trien-7-on) (**IV**) and 7,7-dichlorobicyclo[3.2.0]hept-3-en-6-one (**V**) cleanly react with NH_3 under catalytic conditions to the carboxylic amides **IVa** and **Va**, respectively. **c**, Alkylation of benzylbromide **VI** under catalytic conditions yields monobenzylamnine (**VIa**) and tribenzylamine (**VIb**) in a ratio of 1.0:1.2.

Table 1 | Reaction times, conversions and yields of the catalytic reactions for the substrates I–VI. All reactions were carried out in benzene at RT with p at 1.1 bar of NH_3

Substrate	2 (mol%)	Time (h)	Conversion (%)[a]	Yield (%)[b]
I	20	48	>99	–[c] (**Ia**)
	0		0	0
II	20	20	>99	–[c] (**IIa**)
	0		0	0
III	20	24	>99	72[d] (**IIIa**)
	0		0	0
IV	20	72	>99	49[d] (**IVa**)
	0		0	0
V	20	16	>99	80 (**Va**)
	0		0	0
VI	20	84	49	22.6 (**VIa**), 10.4 (**VIb**)
	0		7	2.6 (**VIa**), 0.2 (**VIb**)

[a]Determined by ^{1}H NMR spectroscopy [b]Determined by ^{1}H NMR spectroscopy against C_6Me_6 as internal standard [c]Oligomerization (for further details see Supplementary Section 1) [d]Preparative yield.

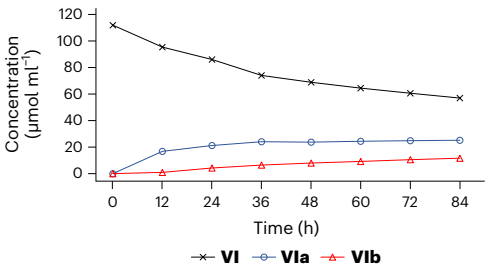

Fig. 4 | Kinetic studies of the catalytic alkylation of benzylbromide. Concentration profiles for the catalytic conversion of benzylbromide **VI** (black) into monobenzylamine **VIa** (blue) and tribenzylamine **VIb** (red) in benzene at RT (compare with Fig. 3c). The concentrations were determined by ^{1}H NMR spectroscopy with C_6Me_6 as internal standard (the error for the concentration determination is estimated to be 5%; error bars not included, one time determination). After 36 h, 21 μmol ml^{-1} of **VIa** can be detected in the reaction mixture and its amount remains almost constant, whereas the concentration of **VIb** slowly increases. After 84 h, a conversion of 49% is reached.

diffraction studies (Fig. 2b) and NMR spectroscopic analysis (Fig. 2c) as the product of the heterolytic splitting of the N–H bond. The P1–C1 (1.8237(12) Å) bond in **3** is slightly elongated by 2 pm compared with **2**, accompanied by a 6 pm elongation of the C5–Al1 (2.0766(12) Å) bond, therefore indicating an increased phosphonium alanate character. Owing to the lack of ring tension, the C5–N1–Al1 angle (110.97(5)°) is 8° wider than in **2**. Even more surprising is the reversibility of this reaction (Fig. 2a). Slow solvent evaporation at room temperature (RT) without applying vacuum leads to quantitative regeneration of **2** (Supplementary Figs. 12 and 13). The crystals of **3** isolated by crystallization under ammonia atmosphere can surprisingly be dried in high vacuum and stored at RT for a month without any sign of decomposition. Dissolving the crystals of **3** in benzene leads to the clean formation of **2** and NH_3, further supporting the reversibility of the NH_3 activation.

In a series of NMR experiments, **2** was reacted with 1 atm of NH_3 in d_6-benzene. As shown in Fig. 2c, the resonance of the *tert*-butyl groups is shifted by 0.3 ppm to lower frequencies (δ_{1H} = 1.34 ppm). This is accompanied by the disappearance of the doublet at δ_{1H} = 1.61 ppm ($^3J_{PH}$ = 21.8 Hz) from the methyl groups at the ylidic carbon atom. A new characteristic resonance for the methyl groups of the protonated ylide carbon is detected at δ_{1H} = 0.92 ppm (doublet of doublets with $^3J_{PH}$ = 18.6 Hz and $^3J_{HH}$ = 6.7 Hz). The associated doublet of septets for the PC*H*$(CH_3)_2$ at δ_{1H} = 1.08 ppm could only indirectly be observed through ^{1}H/^{31}P two-dimensional (2D) NMR experiments, because it suffers from low intensity due to the coupling pattern. By means of ^{1}H^{15}N 2D NMR experiments, the signal detected at δ_{1H} = −0.55 ppm (δ_{15N} = 9.2 ppm) was assigned to the NH_2 group at the aluminium fragment. Additional support for product **3** is the *ortho*-positioned proton of the bridging phenylene entity, which appears at δ_{1H} = 8.66 ppm (compared with δ_{1H} = 8.31 ppm for **2**). In the ^{31}P NMR spectrum, a resonance at

https://doi.org/10.1038/s41557-023-01340-9

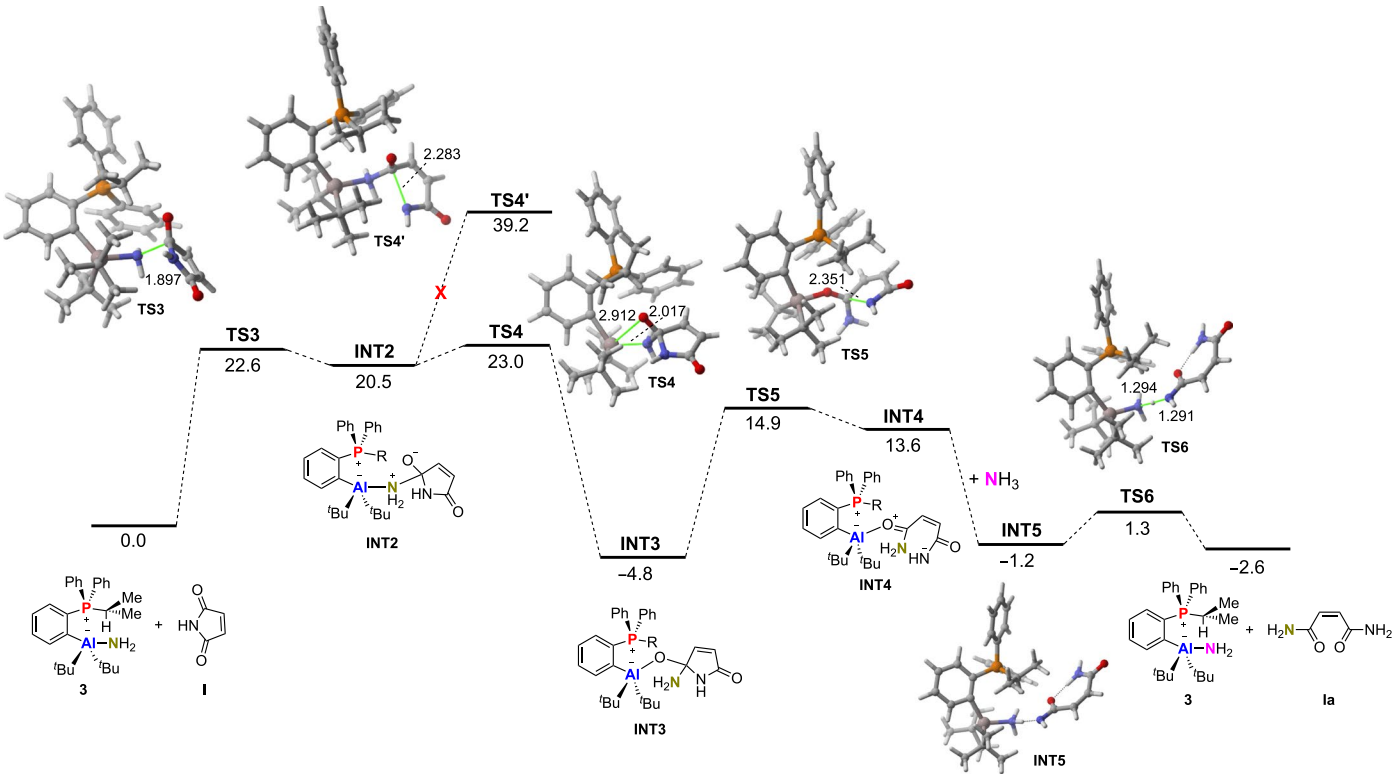

Fig. 5 | Computed reaction profile of the ammonia transfer to Ia. Computed reaction profile (PCM(benzene)-M06-2X/def2-TZVPP//PCM(benzene)-M06-2X/def2-SVP level) for the catalytic ammonia transfer reaction of aluminium–carbon-based ambiphile **2** with NH_3 and maleimide **I**. Relative free energies (ΔG, at 298 K) and bond distances are given in kcal mol^{-1} and angstroms, respectively.

δ_{31P} = 32.9 ppm is observed for **3**, which is shifted by 2.5 ppm to lower frequencies compared with **2**. This can be attributed to the lower electron-withdrawing effect of the aluminium fragment in **3**. To study the reversible reaction in more detail, kinetic studies were performed with isolated **3** in d_6-benzene. The equilibrium was established within 12 h at RT, and resulted in a ratio of **2**:**3** of 0.38:0.62 as indicated by ^{1}H NMR spectroscopy (Supplementary Fig. 23). In the presence of excess of NH_3, this equilibrium was shifted to a ratio of 0.15:0.95 (**2**:**3**) within 5 h. Finally, thermodynamic parameters were determined by van't Hoff analysis (Supplementary Fig. 23). The liberation of NH_3 from **3** is endothermic by $\Delta H°$ = 11.4 ± 0.7 kcal mol^{-1}. Expectedly, this reaction is characterized by a significant positive entropy contribution ($\Delta S°$ = 43.4 ± 2.2 cal mol^{-1} K^{-1}), caused by the liberation of a small molecule (NH_3) concomitant with **2**. These findings are consistent with the calculated values of 16.8 kcal mol^{-1} and 34.3 cal mol^{-1} K^{-1} for ΔH and ΔS, respectively (see below and Fig. 2d).

On the basis of these very promising experimental findings, quantum chemical investigations of the reaction of **2** with NH_3 were carried out at the PCM(benzene)-M06-2X/def2-TZVPP//PCM(benzene)-M06-2X/def2-SVP level of theory (see computational details in Supplementary Section 3), and the corresponding computed reaction profile is depicted in Fig. 2d. Our calculations suggest that the NH_3 activation occurs stepwise. Thus, the transformation begins with the coordination of NH_3 to the aluminium atom and concomitant cleavage of the C_{ylide}–Al bond. The computed reaction barrier of only 19.5 kcal mol^{-1} for transition state **TS1**, furnishing intermediate **INT1**, is compatible with a process occurring at RT. As the second step, this slightly endergonically formed zwitterionic intermediate **INT1** is transformed into the observed species **3** through **TS2**, a saddle point associated with the migration of a hydrogen atom from the coordinate NH_3 moiety to the C_{ylide} atom. The cleavage of the N–H bond requires a comparably low barrier of only 1.6 kcal mol^{-1} in a −4.4 kcal mol^{-1} exergonic transformation. Overall, the computed flat energy profile of the reaction with a relatively small activation barrier of ca. 20 kcal mol^{-1} and a reaction energy of ca. −4 kcal mol^{-1} is in full agreement with the empirically observed reversible NH_3 activation described above and provides further support to the NMR spectroscopy findings.

Catalytic ammonia transfer

Next, we explored the potential of **2** to act as an NH_3 transfer pre-catalyst. Indeed, we found that activated and strained substrates (Fig. 3) reacted with non-aqueous NH_3 in the presence of 20 mol% **2** (which forms **3** in the presence of ammonia). It is important to note that no reactivity was observed in the absence of **2** and otherwise identical non-aqueous conditions. Even though there are already precedents in aqueous ammonia chemistry for the ring-opening reactions shown[44–47], this proof-of-principle study clearly demonstrates for the first time the possibilities for activating and catalytically transforming non-aqueous NH_3. For example, the malimides **I** and **II** were converted into the linear products **Ia** and **IIa** (Fig. 3a), which, however, could not be isolated because they undergo oligomerization once they are formed (for further details, see Supplementary Section 1). Some phosphonium species, which indicate degeneration of the catalyst, could be detected as side products in the ^{31}P{^{1}H} NMR spectra. We assume that the decomposition products initiate the oligomerization of the linear products. Tosylaziridine **III** reacts cleanly with NH_3 under catalytic conditions, leading to ring opening and further deprotonation to form the ammonium salt **IIIa** in 72% yield. Furthermore, the reactions of benzocyclobutenone (bicyclo[4.2.0]octa-1,3,5-trien-7-on) (**IV**) and 7,7-dichlorobicyclo[3.2.0]hept-3-en-6-one (**V**) with NH_3 and 20 mol% **2** furnished the carboxylic amides **IVa** and **Va**, respectively, in quantitative yield according to ^{1}H NMR spectra and in 49% yield after extraction and recrystallization after stirring for 3 days, in the case of **IVa** (Fig. 3b). ~~conversions~~ and yields of all catalytic reactions are summarized in Table 1.

Finally, we turned our attention to the alkylation of NH_3 by benzylbromide (**VI**, Fig. 3c). This reaction is particularly challenging

since, under aqueous conditions, only polyalkylations take place[48–50]. However, the catalytic reaction produced, after quantitative conversion of **VI**, a ratio of 1.0:1.2 of monobenzylamine (**VIa**) and tribenzylamine (**VIb**) after 120 h. As can be seen from Fig. 4, kinetic studies by ^{1}H NMR spectroscopy of the reaction of **VI** in the presence of 20 mol% **2** and NH_3 revealed that the initially formed **VIa** reacts then with BnBr to form Bn_2NH, which upon reaction with another equivalent of BnBr, finally forms Bn_3N (**VIb**). As Bn_2NH could not be detected by NMR spectroscopy, we assume that the reaction with BnBr is comparatively fast. After 36 h, one equivalent of **VIa** can be detected in the reaction mixture and its amount remains almost constant, whereas **VIb** equivalents slowly increase. After 84 h, a conversion of 49% is reached. The fourth substitution is unfavourable due to the decreasing pK_a value, following $BnNH_2$ (9.34) > Bn_2NH (8.52) > Bn_3N (7.44) (ref. 51). In stark contrast, the benzylation of NH_3 in the absence of **2** produces **VIa** and **VIb** in a combined yield of only 7% after 84 h. These reactions clearly show the so far unprecedented catalytic conversion of non-aqueous NH_3 into organic molecules by a main-group element catalyst.

Computational studies

To shed some light on the mechanisms for the ammonia transfer to **I**–**V**, quantum chemical calculations were conducted on the transformation involving **I** as a representative example. As can be seen from the computed reaction profile provided in Fig. 5, the process begins with the nucleophilic addition of the NH_2 moiety of **3** (readily formed upon reaction of **2** and NH_3, see above) to one of the carbonyl groups of maleimide, leading to intermediate **INT2**, with an activation barrier of 22.6 kcal mol^{-1} (via **TS3**). The direct ring opening from **INT2** is, by 39.2 kcal mol^{-1}, kinetically unfeasible. Alternatively, an almost barrierless N-to-O coordination change takes place via **TS4** in a highly exergonic transformation leading to **INT3**. From **INT3**, a much easier, Lewis acid-induced ring opening occurs via **TS5**, leading to intermediate **INT4**. This is followed by transamination and protonation of the product (via **INT5**/**TS6**) with concomitant regeneration of the catalytically active species **3**. Regeneration of **3** as a last step could be confirmed by ^{1}H NMR spectroscopy of the reaction mixture of **III** once the amination reaction is finished (Supplementary Fig. 15).

Conclusion

We present the first example of a main-group element-derived catalyst for the activation and transfer of non-aqueous ammonia. The uncommon combination of an aluminium Lewis acid and adjacent carbon Lewis base in the form of a phosphorus ylide bearing an aluminium fragment in the *ortho* position of a phenyl ring reacts reversibly with ammonia under heterolytic splitting of one N–H bond at ambient conditions. Moreover, the catalytic NH_3 transfer to a variety of electrophiles including maleimide **I**, phenylmaleimide **II**, tosylazirine **III**, cyclobutenones **IV** and **V** and benzylbromide **VI** was demonstrated in the presence of 20 mol% **2**, which in the presence of NH_3, forms the catalytically active NH_3 activation product **3**.

Online content

Any methods, additional references, Nature Portfolio reporting summaries, source data, extended data, supplementary information, acknowledgements, peer review information; details of author contributions and competing interests; and statements of data and code availability are available at https://doi.org/10.1038/s41557-023-01340-9.

References

1. Streiff, S. & Jérôme, F. Hydroamination of non-activated alkenes with ammonia: a holy grail in catalysis. *Chem. Soc. Rev.* **50**, 1512–1521 (2021).
2. Werner, A. Coordination chemistry. *Z. Anorg. Chem.* **3**, 267 (1893).
3. Bezdek, M. J., Guo, S. & Chirik, P. J. Coordination-induced weakening of ammonia, water, and hydrazine X–H bonds in a molybdenum complex. *Science* **354**, 730–733 (2016).
4. Bryan, E. G., Johnson, B. F. G. & Lewis, J. 1,1,2,2,2,2,3,3,3,3-Decacarbonyl-1-(η-cyclohexa-1,3-diene)-triangulo-triosmium: a novel intermediate in synthetic osmium cluster chemistry. *J. Chem. Soc. Dalton Trans*. https://doi.org/10.1039/DT9770001328 (1977).
5. Hillhouse, G. L. & Bercaw, J. E. Reactions of water and ammonia with bis (pentamethylcyclopentadienyl) complexes of zirconium and hafnium. *J. Am. Chem. Soc.* **106**, 5472–5478 (1984).
6. Casalnuovo, A. L., Calabrese, J. C. & Milstein, D. Rational design in homogeneous catalysis. Iridium(I)-catalyzed addition of aniline to norbornylene via nitrogen-hydrogen activation. *J. Am. Chem. Soc.* **110**, 6738–6744 (1988).
7. Holl, M. M. B., Wolczanski, P. T. & Van Duyne, G. D. The ladder structure of $[(tert\text{-}BuCH_2)_2TaN]_5{\cdot}NH_3{\cdot}2C_7H_8$ and its relationship to cubic tantalum nitride.*J. Am. Chem. Soc.* **112**, 7989–7994 (1990).
8. Braun, T. Oxidative addition of NH_3 to a transition-metal complex: a key step for the metal-mediated derivatization of ammonia? *Angew. Chem. Int. Ed.* **44**, 5012–5014 (2005).
9. Zhao, J., Goldman, A. S. & Hartwig, J. F. Oxidative addition of ammonia to form a stable monomeric amido hydride complex. *Science* **307**, 1080–1082 (2005).
10. Nakajima, Y., Kameo, H. & Suzuki, H. Cleavage of nitrogen–hydrogen bonds of ammonia induced by triruthenium polyhydrido clusters. *Angew. Chem. Int. Ed.* **45**, 950–952 (2006).
11. Morgan, E., MacLean, D. F., McDonald, R. & Turculet, L. Rhodium and iridium amido complexes supported by silyl pincer ligation: ammonia N–H bond activation by a [PSiP]Ir complex. *J. Am. Chem. Soc.* **131**, 14234–14236 (2009).
12. Salomon, M. A., Jungton, A.-K. & Braun, T. Activation of ethylene and ammonia at iridium: C–H versus N–H oxidative addition. *J. Chem. Soc. Dalton Trans*. https://doi.org/10.1039/B906189D (2009).
13. Ni, C., Lei, H. & Power, P. P. Reaction of M(II) diaryls (M = Mn or Fe) with ammonia to afford parent amido complexes. *Organometallics* **29**, 1988–1991 (2010).
14. Brown, R. M. et al. Ammonia activation by a nickel NCN–pincer complex featuring a non-innocent N-heterocyclic carbene: ammine and amido complexes in equilibrium. *Angew. Chem. Int. Ed.* **54**, 6274–6277 (2015).
15. Scheibel, M. G. et al. Homolytic N–H activation of ammonia: hydrogen transfer of parent iridium ammine, amide, imide, and nitride species. *Inorg. Chem.* **54**, 9290–9302 (2015).
16. Margulieux, G. W., Bezdek, M. J., Turner, Z. R. & Chirik, P. J. Ammonia activation, H_2 evolution and nitride formation from a molybdenum complex with a chemically and redox noninnocent ligand. *J. Am. Chem. Soc.* **139**, 6110–6113 (2017).
17. LaPierre, E. A., Piers, W. E. & Gendy, C. Redox-state dependent activation of silanes and ammonia with reverse polarity ($PC_{carbene}P$) Ni complexes: electrophilic vs. nucleophilic carbenes. *J. Chem. Soc. Dalton Trans.* **47**, 16789–16797 (2018).
18. Power, P. P. Main-group elements as transition metals. *Nature* **463**, 171–177 (2010).
19. Weetman, C. & Inoue, S. The road travelled: after main-group elements as transition metals. *ChemCatChem* **10**, 4213–4228 (2018).
20. Hansmann, M. M. & Bertrand, G. Transition-metal-like behavior of main group elements: ligand exchange at a phosphinidene. *J. Am. Chem. Soc.* **138**, 15885–15888 (2016).
21. Wang, Y. & Liu, C.-G. The use of main-group elements to mimic catalytic behavior of transition metals I: reduction of dinitrogen to ammonia catalyzed by bis(Lewis base)borylenium diradicals. *Phys. Chem. Chem. Phys.* **22**, 28423–28433 (2020).

22. Frey, G. D., Lavallo, V., Donnadieu, B., Schoeller, W. W. & Bertrand, G. Facile splitting of hydrogen and ammonia by nucleophilic activation at a single carbon center. *Science* **316**, 439–441 (2007).
23. Wang, Y. et al. Activation of ammonia by a carbene-stabilized dithiolene zwitterion. *J. Am. Chem. Soc.* **144**, 16325–16331 (2022).
24. Yang, X. et al. Radical activation of N–H and O–H bonds at bismuth(II). *J. Am. Chem. Soc.* **144**, 16535–16544 (2022).
25. Abbenseth, J., Townrow, O. P. E. & Goicoechea, J. M. Thermoneutral N–H bond activation of ammonia by a geometrically constrained phosphine. *Angew. Chem. Int. Ed.* **60**, 23625–23629 (2021).
26. Welch, G. C., Juan, R. R. S., Masuda, J. D. & Stephan, D. W. Reversible, metal-free hydrogen activation. *Science* **314**, 1124–1126 (2006).
27. Stephan, D. W. & Erker, G. Frustrated Lewis pairs: metal-free hydrogen activation and more. *Angew. Chem. Int. Ed.* **49**, 46–76 (2010).
28. Stephan, D. W. Frustrated Lewis pairs. *J. Am. Chem. Soc.* **137**, 10018–10032 (2015).
29. Stephan, D. W. Frustrated Lewis pairs: from concept to catalysis. *Acc. Chem. Res.* **48**, 306–316 (2015).
30. Stephan, D. W. & Erker, G. Frustrated Lewis pair chemistry: development and perspectives. *Angew. Chem. Int. Ed.* **54**, 6400–6441 (2015).
31. Stephan, D. W. The broadening reach of frustrated Lewis pair chemistry. *Science* **354**, aaf7229 (2016).
32. Mahdi, T. & Stephan, D. W. Frustrated Lewis pair catalyzed hydroamination of terminal alkynes. *Angew. Chem. Int. Ed.* **52**, 12418–12421 (2013).
33. Mahdi, T. & Stephan, D. W. Stoichiometric and catalytic inter- and intramolecular hydroamination of terminal alkynes by frustrated Lewis pairs. *Chem. Eur. J.* **21**, 11134–11142 (2015).
34. Ma, G., Song, G. & Li, Z. H. Designing metal-free frustrated Lewis pairs catalyst for the efficient dehydrogenation of ammonia borane. *Chem. Eur. J.* **24**, 13238–13245 (2018).
35. Zhang, L. et al. Catalytic dehydrogenation of ammonia borane mediated by a Pt(0)/borane frustrated Lewis pair: theoretical design. *ChemPhysChem* **21**, 2573–2578 (2020).
36. Sarbajna, A., Swamy, V. S. V. S. N. & Gessner, V. H. Phosphorus-ylides: powerful substituents for the stabilization of reactive main group compounds. *Chem. Sci.* **12**, 2016–2024 (2021).
37. Krämer, F., Radius, M., Hinz, A., Dilanas, M. E. A. & Breher, F. Accessing cationic α-silylated and α-germylated phosphorus ylides. *Chem. Eur. J.* **28**, e202103974 (2022).
38. Schier, A. & Schmidbaur, H. Derivatives and coordination compounds of triphenylphosphonium cyclopropylide $(C_6H_5)_3P{=}C(CH_2)_2$. *Z. Naturforsch. B* **37**, 1518–1523 (1982).
39. Dureen, M. A. & Stephan, D. W. Biphenylamide ligand complexes of Li and Al: hemilabile arene donors? *J. Chem. Soc. Dalton Trans.* https://doi.org/10.1039/B801772G (2008).
40. Swarnakar, A. K. et al. Application of the donor–acceptor concept to intercept low oxidation state group 14 element hydrides using a Wittig reagent as a Lewis base. *Inorg. Chem.* **53**, 8662–8671 (2014).
41. Korth, K. & Sundermeyer, J. Interaction of t-butyllithium and triphenylmethylenephosphoranes. *Tetrahedron Lett.* **41**, 5461–5464 (2000).
42. Radius, M. & Breher, F. α-Borylated phosphorus ylides (α-BCPs): electronic frustration within a C–B π-bond arising from the competition for a lone pair of electrons. *Chem. Eur. J.* **24**, 15744–15749 (2018).
43. Wiberg, N. *Lehrbuch der Anorganischen Chemie*. 102nd edn (W. de Gruyter, 2007).
44. Brook, P. R. & Duke, A. J. Ring-opening reactions of 7,7-dichlorobicyclo[3,2,0]hept-2-en-6-one and its conversion into methyl benzoate with methoxide ion. *J. Chem. Soc. C* https://doi.org/10.1039/J39710001764 (1971).
45. Roedig, A., Bonse, G., Ganns, E. M. & Heinze, H. Der einfluss der perchlorsubstitution auf einige ringöffnungsreaktionen des benzocyclobutendions. *Tetrahedron* **33**, 2437–2440 (1977).
46. Argouarch, G., Stones, G., Gibson, C. L., Kennedy, A. R. & Sherrington, D. C. Bifurcated, modular syntheses of chiral annulet triazacyclononanes. *Org. Biomol. Chem.* **1**, 4408–4417 (2003).
47. Zhang, L. et al. Iridium-catalyzed asymmetric hydrogenation of simple ketones with tridentate PNN ligands bearing unsymmetrical vicinal diamines. *J. Org. Chem.* **88**, 2942–2951 (2023).
48. Kim, J., Kim, H. J. & Chang, S. Synthetic uses of ammonia in transition-metal catalysis. *Eur. J. Org. Chem.* **2013**, 3201–3213 (2013).
49. Lawrence, S. A. *Amines: Synthesis, Properties and Applications* (Cambridge Univ. Press, 2005).
50. Legnani, L., Bhawal, B. N. & Morandi, B. Recent developments in the direct synthesis of unprotected primary amines. *Synthesis* **49**, 776–789 (2017).
51. Tshepelevitsh, S. et al. On the basicity of organic bases in different media. *Eur. J. Org. Chem.* **2019**, 6735–6748 (2019).

Methods

General methods

All operations were carried out under dry argon using standard Schlenk and glovebox techniques. ~~*Tert*-~~BuLi (1.7 M in pentane) was used as purchased from Sigma-Aldrich. The ylide Ph_3PCMe_2 and *t*-Bu_2AlCl were synthesized according to literature procedures[40,52]. Solvents were dried over Na/K and rigorously degassed before use. NMR spectra were recorded on Bruker Avance Neo 400 or an Avance 300 spectrometer operating at ^1H Larmor frequencies of 400 or 300 MHz in dry degassed deuterated solvents. For the kinetic studies, we used a Migratek Spinsolve 80 benchtop NMR spectrometer. The ^1H, $^{13}C\{^1H\}$ and ^{29}Si chemical shifts are reported against tetramethylsilane, and $^{31}P\{^1H\}$ against H_3PO_4. Coupling constants (*J*) are given in hertz as positive values, regardless of their real individual signs. The multiplicity of the signals is indicated as s, d, q, sept or m for singlet, doublet, quartet, septet or multiplet, respectively. The assignments were confirmed, as necessary, with the use of 2D NMR correlation experiments. Infra-red spectra were measured on a Bruker Alpha spectrometer using the attenuated reflection technique (ATR), and the data are reported in wavenumbers (cm^{-1}). The intensity of the absorption band is indicated as vw (very weak), w (weak), m (medium), s (strong), vs (very strong) and br (broad). Melting points were measured with a Thermo Fischer melting point apparatus and are not corrected. Elemental analyses were carried out in the institutional technical laboratories of the Karlsruhe Institute of Technology (KIT). High-resolution mass spectra were measured at the Institute of Organic Chemistry at KIT on a Thermo Fisher Orbitrap. Matrix-assisted laser desorption/ionization mass spectra were measured at the Institute of Organic Chemistry at KIT on a Shimadzu Axima Confidence with 6-aza-2-thiothymine (143.17 g mol^{-1}) as matrix.

(2-Li-C_6H_4)ph_2PCMe_2. In a glovebox, Ph_3PCMe_2 (5.00 g, 16.43 mmol) was placed in toluene (30 ml). Solid *t*-BuLi (1.05 g, 16.43 mmol) was added to the red solution at RT, resulting in a brightening of the reaction mixture and the formation of a yellow precipitate. Stirring overnight followed by filtering and drying the precipitate in high vacuum afforded **1** as an extremely air-sensitive yellow powder (2.4 g, 47%). Next, **1** was used for the following syntheses without further purification. Note that **1** decomposes slowly in tetrahydrofuran and in the glovebox at RT, but can be stored at −30 °C for months.

M.p.: decomposition 75 °C. ^1H NMR (300 MHz, 298 K, C_6D_6, ppm): δ = 8.29–8.21 (m, H_{PhLi_ortho}, 1H), 7.69–7.57 (m, HH_{Ar}, 5H), 7.10–6.95 (m, H_{Ar}, 9H), 1.96 (d, $^3J_{PH}$ = 21.8 Hz, H_{CMe2}, 6H). $^{31}P\{^1H\}$ NMR (121 MHz, 298 K, C_6D_6, ppm): δ = 21.1 (s). ^7Li NMR (116 MHz, 298 K, C_6D_6, ppm): δ = 4.3 (s).

(2-{Al*t*-Bu_2}-C_6H_4)Ph_2PCMe_2. In a vial in a glovebox, *t*-Bu_2AlCl (263 mg, 1.49 mmol) was placed in toluene (10 ml) and solid **1** (462 mg, 1.49 mmol) was added. While stirring for 30 min, the reaction mixture became lighter in colour to light orange. The reaction mixture was filtered through a syringe filter, and the solvent was removed under reduced pressure. Hexane (5 ml) was added to the light-red high-viscosity oil, and the mixture was briefly heated. Then, the slightly red, slightly turbid solution was stored at −30 °C overnight. The mother liquor was decanted from the resulting precipitate. After drying under a high vacuum and washing with hexane (3 × 5 ml), the residue was taken up in toluene (10 ml), concentrated and mixed with hexane (5 ml). The **2** crystallized from this mixture in the form of colourless blocks (180 mg, 28%). The mother liquor and wash solution were combined and stored at −30 °C overnight. This yielded additional **2** (167 mg, 26%) in the form of colourless blocks.

M.p.: 165 °C. ^1H NMR (300 MHz, 298 K, C_6D_6, ppm): δ = 8.35–8.37 (m, H_{PhAl_ortho}, 1H), 7.39–7.36 (m, H_{PhAl_meta}, 1H), 7.36–7.33 (m, H_{PhAl_meta}, 1H), 7.33–7.30 (m, H_{Ph2_para}, 2H), 7.30–7, 27 (m, H_{PhAl_para}, 1H), 7.11–6.94 (m, H_{Ph2_meta}, 4H), 6.94–6.82 (m, H_{Ph2_ortho}, 4H), 1.61 (d, $^3J_{PH}$ = 21.8 Hz, H_{CMe2}, 6H), 1.31 (s, H_{CMe3}, 18H). $^{13}C\{^1H\}$ NMR (75 MHz, 298 K, C_6D_6, ppm): δ = 139.3 (d, $^2J_{PC}$ = 20.9 Hz, C_{PhAl_ortho}), 134.6 (d, $^4J_{PC}$ = 7.6 Hz, C_{PPh2_para}) 133.3 (d, $^2J_{PC}$ = 14.41 Hz, C_{PPh2_ortho}), 131.9 (d, $^4J_{PC}$ = 2.9 Hz, C_{PhAl_para}), 131.4 (d, $^1J_{PC}$ = 104.9 Hz, C_{PPh2_ipso}), 131.2 (d, $^3J_{PC}$ = 3.5 Hz, C_{PhAl_meta}), 128.6 (d, $^3J_{PC}$ = 10.6 Hz, C_{PPh2_meta}), 126.8 (d, $^3J_{PC}$ = 12.8 Hz, C_{PhAl_meta}), 124.6 (d, $^1J_{PC}$ = 60.0 Hz, C_{CMe2}), 33.3 (s, C_{CMe3}), 24.6 (d, $^2J_{PC}$ = 3.8 Hz, C_{CMe2}). $^{*31}P\{^1H\}$ NMR (121 MHz, 298 K, C_6D_6, ppm): δ = 35.4 (s). IR (ATR, cm^{-1}): $\tilde{\upsilon}$ = 2,955 (vw), 2,923 (vw), 2,803 (m), 2,685 (vw), 2,133 (vw), 1,485 (vw), 1,462 (w), 1,438 (w), 1,379 (vw), 1,351 (vw), 1,243 (vw), 1,162 (vw), 1,098 (m), 1,028 (vw), 999 (vw), 929 (vw), 882 (w), 808 (m), 754 (w), 734 (w), 721 (w), 712 (w), 697 (vs), 657 (m), 635 (s), 556 (vs), 533 (vs), 511 (s), 476 (w), 453 (s), 433 (vw), 412 (m), 391 (vw). Elemental analysis (%): (calculated) found for $C_{29}H_{38}AlP$: C (78.35) 77.85, H (8.62) 8.52. ~~*M/z*~~ (electrospray ionization) (calculated: 444.25, found M(H^+): 445.29535). *The signals for the tertiary carbon atoms Ph_{Al_ipso}, Ph_{Al_ortho} and C_{Me3} could not be detected in the $^{13}C\{^1H\}$ NMR.

(2-{Al(NH_2)*t*-Bu_2}-C_6H_4)$Ph_2PC(H)Me_2$. For characterization in solution, **2** was dissolved in C_6D_6 (0.6 ml) and degassed. Subsequently, 1.1 bar NH_3 was applied and the reaction mixture was stored overnight at RT and then NMR spectroscopically characterized (allowing the solvent to slowly evaporate gave back **2**). For crystallization of **3** under an NH_3 atmosphere, **2** (50 mg, 0.12 mmol) was placed in toluene (2 ml) in a Schlenk flask. On top of this flask, a Schlenk frit equipped with a Young flask containing hexane was mounted in converse orientation (Supplementary Fig. 1). The whole apparatus was degassed and flooded with NH_3 (1.1 bar). The reaction mixture was stirred overnight. Then, the hexane was poured slowly onto the frit to overlay the reaction mixture. The **3** crystallized within a few days in the form of small colourless needles. Removing the mother liquor and drying the residue in high vacuum yielded **3** along with 10% **2**. Dissolving the crystals of **3** in benzene led to the formation of **2** and NH_3.

M.p.: 133 °C. ^1H NMR (300 MHz, 298 K, C_6D_6, ppm): δ = 8.69–8.63 (m, H_{PhAl_ortho}, 1H), 7.36–7.25 (m, H_{PhAl_meta}, H_{PhAl_meta}, H_{Ph2_para}, H_{PhAl_para}, 5H), 7.05–6.94 (m, H_{Ph2_meta}, 4H), 6.93–6.84 (m, H_{Ph2_ortho}, 4H), 1.34 (s, H_{CMe3}, 18H), 0.92 (dd, $^3J_{PH}$ = 18.7 Hz, $^3J_{HH}$ = 6.6 Hz, H_{CMe2}, 6H), −0.55 (s, NH_2, 2H). $^{*13}C\{^1H\}$ NMR (75 MHz, 298 K, C_6D_6, ppm): δ = 143.3 (d, $^2J_{PC}$ = 24.5 Hz, C_{PhAl_ortho}), 134.5 (d, $^4J_{PC}$ = 8.2 Hz, C_{PPh2_para}) 133.4 (d, $^2J_{PC}$ = 13.3 Hz, C_{PPh2_ortho}), 132.9 (d, $^4J_{PC}$ = 2.8 Hz, C_{PhAl_para}), 129.3 (d, $^3J_{PC}$ = 4.0 Hz, C_{PhAl_meta}), 129.3 (d, $^3J_{PC}$ = 11.3 Hz, C_{PPh2_meta}), 126.4 (d, $^1J_{PC}$ = 88.4 Hz, C_{PPh2_ipso}), 125.3 (d, $^3J_{PC}$ = 13.2 Hz, C_{PhAl_meta}), 121.9 (d, $^1J_{PC}$ = 78.4 Hz, C_{CMe2}), 33.7 (s, C_{CMe3}), 17.7 (d, $^2J_{PC}$ = 2.6 Hz, C_{CMe2}). $^{*31}P\{^1H\}$ NMR (121 MHz, 298 K, C_6D_6, ppm): δ = 32.9 (s). $^1H/^{15}N$ HMBC NMR (298 K, C_6D_6, ppm): δ = −0.55/9.2 (NH_2). *The proton at the ylidic carbon atom could not be detected in the ^1H NMR. The signals for the tertiary carbon atoms Ph_{Al_ipso}, Ph_{Al_ortho} and C_{Me3} could not be detected in the $^{13}C\{^1H\}$ NMR.

Catalysis

For the catalytic ammonia transfer reactions, **2** (20 mol%) and either **I** (112 mg, 1.16 mmol), **II** (96 mg, 0.56 mmol), **III** (88.7 mg, 0.45 mmol) or **IV** (271 mg, 2.3 mmol) were placed in a Young flask in benzene (8 ml) and the mixtures were degassed. Subsequently, the reaction mixtures were gassed with NH_3 (1.1 bar) and stirred at RT for 1 week for **I** and 3 days for **II**–**IV**. Reactions involving **V** (9.6 mg, 0.056 mmol) and **VI** (19.9 mg, 0.11 mmol) were performed at NMR scale with C_6Me_6 as internal standard. Control reactions without catalyst under otherwise identical conditions gave no or poor conversions.

Isolation of the oligomerization products of **Ia** and **IIa**: The oligomers were separated by filtration. After drying under high vacuum, they were applied for further analysis (for further details see Supplementary Section 1).

Isolation of **IIIa**: While stirring the reaction mixture, a colourless solid precipitated. Collection by filtration and drying under high vacuum yielded **IIIa** (75 mg, 72%). ^1H NMR (300 MHz, 298 K $CDCl_3$, ppm): δ = 7.82 (d, $^3J_{HH}$ = 8.0 Hz, $H_{Ar,}$ 2H), 7.26 (d, $^3J_{HH}$ = 8.0 Hz, H_{Ar}, 2H), 3.34 (s, H_{CH2}, 4H), 2.38 (s, H_{Me}, 3H). *M/z* (electrospray ionization) (calculated: 231.10, found: 231.11893).

Isolation of the product **IVa**: While stirring the reaction mixture, a colourless precipitate formed. It was separated by filtration and dried under high vacuum to yield **IVa** (122 mg, 39%). The solvent of the filtrate was removed under reduced pressure. The residue was extracted with benzene (2 ml), and pentane (5 ml) was added. The colourless precipitate was collected by filtration and dried in vacuo. The remaining solid was extracted with $CHCl_3$. Removing the solvent and recrystallization from EtOH (2 ml) yielded additional **IVa** (31 mg, 10%). The ^{1}H NMR spectrum in CD_2Cl_2 corresponds to the literature[53].

Yield determination of **Va**: **Va** precipitates from d_6-benzene during the reaction. To determine the yield, the reaction mixture was dried under a high vacuum and dissolved in $CDCl_3$. ^{1}H NMR (300 MHz, 298 K, $CDCl_3$, ppm): δ = 6.05 (m, H_{CH}, 1H); 5.89 (m, H_{CH}, overlap with H_{NH2}, 1H); 6.38 (d, H_{CH}, 1H) 5.79 (bs, H_{NH2}, 2H); 3.24 (m, H_{CH}, 1H); 2.69 (m, H_{CH2}, 2H).

Data availability

The data that support the findings of this study are available within the paper and its Supplementary Information. Raw and unprocessed NMR, HRMS and gel permeation chromatography data are available from figshare (https://doi.org/10.6084/m9.figshare.22357168)[54]. Materials and methods, computational studies including cartesian coordinates and energies for the computed structures, experimental procedures, characterization data, NMR spectra and mass spectrometry data are available in the paper with further details in the Supplementary Information. Crystallographic data for the structures reported in this article have been deposited at the Cambridge Crystallographic Data Centre, under deposition numbers 2180947 (**2**) and 2180948 (**3**). For further crystallographic details see Supplementary Section 2. Copies of the data can be obtained free of charge via https://www.ccdc.cam.ac.uk/structures/. Source data are provided with this paper.

References

52. Uhl, W., Wagner, J., Fenske, D. & Baum, G. *N,N,N′,N′*-Tetramethylethylendiamin-di(tert-butyl)aluminium-Kationen—Molekülstruktur des $[(Me_3C)_2Al \cdot TMEDA]^{\oplus}[(Me_3C)_2AlBr_2]^{\ominus}$ *Z. Anorg. Allg. Chem.* **612**, 25–34 (1992).
53. Allen, C. L., Burel, C. & Williams, J. M. J. Cost efficient synthesis of amides from oximes with indium or zinc catalysts. *Tetrahedron Lett.* **51**, 2724–2726 (2010).
54. Krämer, F., Paradies, J., Fernández, I. & Breher, F. A crystalline aluminum–carbon-based ambiphile capable of activation and catalytic transfer of ammonia in non-aqueous media. Preprint at ChemRxiv https://doi.org/10.6084/m9.figshare.22357168 (2023).

Acknowledgements

This work was partly carried out with the support of the Karlsruhe Nano Micro Facility, a Helmholtz research platform at KIT, and we thank D. Fenske, A. Hinz and B. Birenheide for help with X-ray diffraction. We also thank K. Kohnle, A. Mösle, L. Hirsch and A. Hochgesand from the Institute of Organic Chemistry at KIT for performing mass spectral and elemental analysis. R. Nickisch and L. Santos Correa from the Institute of Organic Chemistry at KIT are acknowledged for their help with gel permeation chromatography measurements. The authors acknowledge support by the state of Baden-Württemberg through bwHPC and the German Research Foundation through grant no INST 40/575-1 FUGG (JUSTUS 2 cluster). I.F. is grateful to the Spanish MCIN/AEI/10.13039/501100011033 (grants PID2019-106184GB-I00 and RED2018-102387-T). The authors received no specific funding for this work.

Author contributions

F.B. supervised the project. I.F. performed the quantum chemical calculations. J.P. supported the catalytic studies and the van't Hoff analysis. F.K. conducted all experiments and wrote the manuscript with input from all authors.

Competing interests

The authors declare no competing interest.

Additional information

Supplementary information The online version contains supplementary material available at https://doi.org/10.1038/s41557-023-01340-9.

Correspondence and requests for materials should be addressed to Frank Breher.

Peer review information *Nature Chemistry* thanks Cameron Jones and the other, anonymous, reviewer(s) for their contribution to the peer review of this work.

QUERY FORM

Manuscript ID	**[Art. Id: 1340]**
Author	**Felix Krämer**

AUTHOR:

The following queries have arisen during the editing of your manuscript. Please answer by making the requisite corrections directly in the e.proofing tool rather than marking them up on the PDF. This will ensure that your corrections are incorporated accurately and that your paper is published as quickly as possible.

Query No.	*Nature of Query*
Q1:	Since the references were not cited in numerical order, they have been renumbered in the order of appearance. Please check.
Q2:	Please check your article carefully, coordinate with any co-authors and enter all final edits clearly in the eproof, remembering to save frequently. Once corrections are submitted, we cannot routinely make further changes to the article.
Q3:	Note that the eproof should be amended in only one browser window at any one time; otherwise changes will be overwritten.
Q4:	Author surnames have been highlighted. Please check these carefully and adjust if the first name or surname is marked up incorrectly, as this will affect indexing of your article in public repositories such as PubMed. Also, carefully check the spelling and numbering of all author names and affiliations, and the corresponding author(s) email address(es). Please note that email addresses should only be included for designated corresponding authors, and you cannot change corresponding authors at this stage except to correct errors made during typesetting.
Q5:	You cannot alter accepted Supplementary Information files except for critical changes to scientific content. If you do resupply any files, please also provide a brief (but complete) list of changes. If these are not considered scientific changes, any altered Supplementary files will not be used, only the originally accepted version will be published.
Q6:	In the e.proof tool, the numbers for those compounds that will be deposited in PubChem do not appear bold, and the link is not visible. You do not need to amend this, they will appear correctly once published online.
Q7:	Please check Figures for accuracy as they have been relabelled. Please markup minor changes in the eProof. For major changes, please provide revised figures. (Please note that in the eProof the figure resolution will appear at lower resolution than in the pdf and html versions of your paper.)
Q8:	If applicable, please ensure that any accession codes and datasets whose DOIs or other identifiers are mentioned in the paper are scheduled for public release as soon as possible, we recommend

QUERY FORM

Manuscript ID	**[Art. Id: 1340]**
Author	**Felix Krämer**

AUTHOR:

The following queries have arisen during the editing of your manuscript. Please answer by making the requisite corrections directly in the e.proofing tool rather than marking them up on the PDF. This will ensure that your corrections are incorporated accurately and that your paper is published as quickly as possible.

Query No.	*Nature of Query*
	within a few days of submitting your proof, and update the database record with publication details from this article once available.
Q9:	In the Main text, please provide a sentence starting "In this Article..." that provides a brief description of the paper.
Q10:	In the sentence starting "Surprisingly, although the open form of 2 is..." please confirm the expansion of DFT.
Q11:	Please confirm the u[illegible] of cal mol-1 K-1 where applied.
Q12:	In Table 1 and Fig. 3, please define *p*.
Q13:	In the sentence starting "1H, 13C{1H} and 29Si chemical shifts were..." please confirm the expansion of TMS.
Q14:	In the sentence starting "Matrix-assisted laser desorption/ionization mass spectra were measured ..." please confirm the expansion of MALDI.
Q15:	In the sentence starting "Next, 1 was used for the following syntheses without further..." please confirm the expansion of THF.
Q16:	In the sentence starting "Elemental analysis (%)..." please confirm the expansion of calcd.
Q17:	In the sentence starting "M/z (electrospray ionization)..." please confirm the expansion of ESI.
Q18:	In the sentence starting "$^{1}H/^{15}N$ HMBC NMR (298 K, C_6D_6, [illegible] m)..." please expand HMBC.
Q19:	In the sentence starting "R. Nickisch and L. Santos Correa from the Institute of Organic Chemistry..." please confirm the expansion of GPC.
Q20:	For ref. 2, please add the final pag[illegible]mber or confirm that it is a single-page reference.

QUERY FORM

Manuscript ID	**[Art. Id: 1340]**
Author	**Felix Krämer**

AUTHOR:

The following queries have arisen during the editing of your manuscript. Please answer by making the requisite corrections directly in the e.proofing tool rather than marking them up on the PDF. This will ensure that your corrections are incorporated accurately and that your paper is published as quickly as possible.

Query No.	*Nature of Query*
Q21:	If ref. 54 (preprint) has now been published in final peer-reviewed form, please update the reference details if appropriate.